Preparation, Characterization, and Unusual Reactivity of Fe-MCM-41†

Michael Stockenhuber,*,‡ Michael J. Hudson,§ and Richard W. Joyner‡

Catalysis Research Laboratory, Department of Chemistry and Physics, Nottingham Trent University, Clifton Lane, Nottingham NG11 8NS, U.K., and Department of Chemistry, University of Reading, Whiteknights, Reading RG6 6AD, U.K.

Received: September 20, 1999; In Final Form: January 4, 2000

A new preparation method for highly dispersed iron in mesoporous MCM-41 materials has been developed, employing a methanolic solution of iron(III) nitrate. In situ EXAFS and NO adsorption followed by IR spectroscopy suggest that the resulting iron is present mainly in the form of isolated cations bound to the internal surface of the purely siliceous host material. Interchange between the Fe(II)/Fe(III) redox pair is facile, depending on the way in which the material is treated. The preparation procedure not only generates these highly dispersed iron species but also results in the formation of methoxy groups strongly bound to the MCM-41. It is suggested that the iron cations are chemically bound through siloxane bridges at silanol nests within the porous framework of the MCM-41 material.

1. Introduction

Iron-exchanged microporous materials have been successfully used in a number of catalytic applications. Fe-ZSM-5 zeolite is active for oxidation of hydrocarbons with N_2O[1,2] and is a very stable and active catalyst for selective catalytic reduction of NO_x with hydrocarbons.[3,−6] In addition, we found that incorporation of iron into ZSM-5 leads to the formation of very unusual iron−oxygen *nanoclusters*, which are extremely stable against reduction to metallic iron.[7,8] The use of microporous materials, however, restricts the potential catalytic application to relatively small reactant molecules. To be able to utilize the iron catalytic site for larger molecules in fine chemical applications, it may be advantageous to increase the pore sizes of the host molecular sieve structure, so we now present results for purely siliceous MCM-41, which has a channel diameter of ca. 30 Å.

The complex aqueous chemistry of iron means that ion exchange into porous materials is generally difficult. For mesoporous materials it has even been suggested that, due to their larger pore sizes, only extended iron oxide species can be introduced.[9] Though transition metals have been successfully introduced into microporous aluminosilicates by several different methods, including ion exchange,[10−12] solid-state ion exchange,[13,14] and impregnation,[15,16] only a handful of reports deal with the introduction of transition metal cations into MCM-41 after synthesis.[17−19] In cobalt nitrate impregnated MCM-41, mainly larger particle sizes with up to 45 cobalt atoms per particle were found. Introduction of cobalt leads to small cobalt oxide clusters on the walls of MCM-41, which exhibited some activity in the selective catalytic reduction of nitrogen oxides in the presence of water.[20] Attempts have been made to introduce heteropolyacids,[21] and some transition metal complexes[22] have been grafted onto MCM-41 materials after synthesis.

In the following, we report on the successful incorporation of highly dispersed iron species from methanolic solution into purely siliceous MCM-41 and discuss the structure, redox stability, and reactivity of the resulting materials. Methanol has been used as a solvent, as MCM-41 is reported to be unstable in water,[23] since relatively high concentrations of iron can be dissolved in methanol and because we have been able successfully to introduce well-dispersed iron into ZSM-5 zeolite in this way.[8] This recently published, detailed study of the preparation, structure, and properties of Fe-ZSM-5 serves to illuminate many of results on Fe-MCM-41 reported here.

2. Experimental Section

2.1. Preparation Procedures. Purely siliceous MCM-41 was prepared according to a preparation procedure described in detail by Grün et al.[24] Iron was introduced from a methanolic solution of iron(III) nitrate nonahydrate (80 g L^{-1}). The solution (100 mL) was filtered into a flask containing MCM-41 (2 g), and the resulting mixture was stirred while argon was bubbled through the solution at a flow rate of 35 mL min^{-1}. After 24 h the solution was filtered under reduced pressure, washed with methanol, and dried at 373 K.

2.2. Characterization. The prepared MCM-41 samples have been characterized by transmission electron microscopy, nitrogen physisorption, and low-angle X-ray diffraction, and details of these procedures are given by Hudson et al.[25] The iron content of the materials was determined by atomic absorption spectroscopy, and the iron-containing samples were subsequently characterized by temperature-programmed reduction, in situ X-ray absorption spectroscopy (EXAFS and XANES), and infrared spectroscopy. Full details of these characterization procedures have been given previously.[8]

3. Results and Discussion

Electron microscope images of the prepared MCM-41 showed the presence of the expected well-defined, hexagonal porous arrays, and low-angle X-ray diffraction studies of the same material have a peak at $2\theta = 1°$, indicative of a mean pore size

† Part of the special issue "Gabor Somorjai Festschrift".

* Corresponding author.

‡ Nottingham Trent University. Stockenhuber: Tel/Fax, 44-115-948-6694; E-mail, michael.stockenhuber@ntu.ac.uk. Joyner: Tel, 44-115-948-6837; Fax, 44-115-948-6838; E-mail, richard.joyner@ntu.ac.uk.

§ University of Reading. Tel/Fax: 44-118-931-6717. E-mail: M.J.Hudson@reading.ac.uk.

10.1021/jp993355h CCC: $19.00
Published on Web 04/06/2000

TABLE 1: Iron Content, Surface Area, and TPR Results

catalyst designation (see text)	iron content, wt %	BET surface area, m^2/g	H_2 consumption from TPR, mol of H_2/mol of Fe	
			peak at 675 K	peak at 1014 K
MCM-41	0	960	–	–
Fe-MCM-41 (N_2)	2.92	930	0.26	−0.49
Fe-MCM-41 (air)	2.92	–	0.38	–

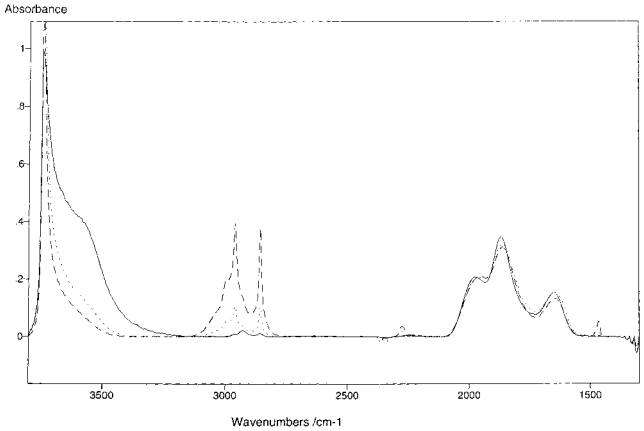

Figure 1. Infrared spectra measured at 425 K of Fe-MCM-41 (dashed line), MCM-41 activated in vacuo at 775 K (solid line), and Fe-MCM-41 activated in O_2 (dotted line).

of ca. 30 Å. The surface area is 960 $m^2\ g^{-1}$, which is typical of MCM-41 materials, and it is not significantly reduced after treatment with methanol or the introduction of iron, as indicated in Table 1. The infrared spectrum of the synthesized MCM-41 material shown in Figure 1 exhibits a peak at 3746 cm^{-1} and a broad band centered at ca. 3600 cm^{-1}. Following assignments that are well attested for zeolites, the sharp feature at 3746 cm^{-1} is attributed to stretching vibrations of terminal SiOH groups, whereas the broad band is due to silanol groups with significant hydrogen-bonding interactions,[26] often called silanol nests. Overtone bands of lattice vibrations occur at 1980, 1872, and 1657 cm^{-1}, and we have used the two higher frequency bands to normalize for wafer thickness, to allow comparative spectral analysis. The concentration of hydroxyl groups, and particularly silanol nests, is much higher in this MCM-41 material than is typically observed in H-ZSM-5.[7]

As shown in Table 1, almost 3% weight of iron is introduced into MCM-41 by a single interaction with the methanolic iron solution, compared to a maximum of <1% that is introduced into H-ZSM-5 by a triple-exchange procedure.[8] Iron is present in significant excess in the preparation liquor, so the uptake is determined by the number of sites available in the MCM-41 material. Infrared spectra show that the methanol solvent also interacts strongly with MCM-41. Figure 1 compares the spectrum of an Fe-MCM-41 sample with that of the prepared, activated MCM-41. The Fe-MCM-41 spectrum exhibits additional bands in the C−H stretching vibration region, at 2857, 2958, and 2995 cm^{-1}. These bands are identical to those observed when methanol interacts with ZSM-5, forming adsorbed methoxy groups.[27] The higher frequency bands are attributed to the antisymmetric stretching vibrations of the CH_3 group and the band at 2857 cm^{-1} is associated with the symmetric mode.[28]

Although we first observed the methoxy species after introduction of iron from methanolic solution, separate experiments showed that stirring the calcined, template-free MCM-41 in methanol generates the same new bands in the hydrocarbon region as stirring the material in a methanolic iron nitrate solution. The methoxy groups do not come from the organic template used in the synthesis of MCM-41, since only an insignificant concentration of hydrocarbon species is found in the synthesized sample. The methoxy species are very stable, and their intensity could be substantially reduced only by prolonged heating in oxygen at $T > 800$ K.

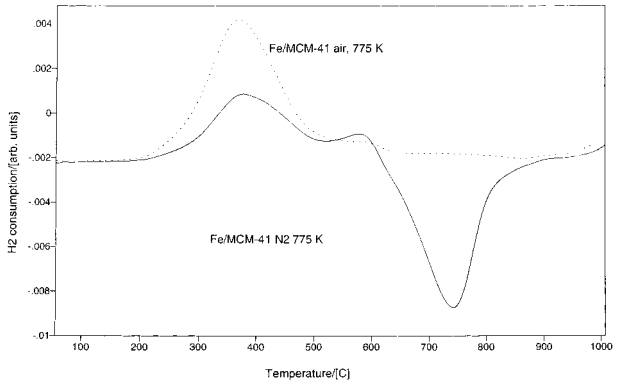

Figure 2. Temperature-programmed reduction results for Fe-MCM-41 activated at 775 K in nitrogen and in air. The negative feature at ca. 740 K for the nitrogen-activated sample is the result of hydrogen evolution.

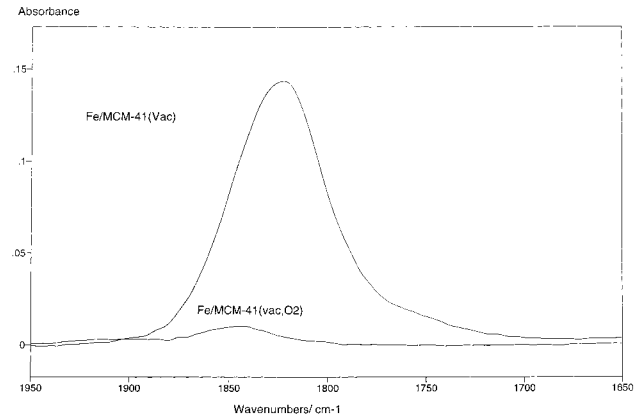

Figure 3. Influence of pretreatment conditions on NO adsorption; infrared spectra measured under 1 mbar NO for Fe-MCM-41 activated in vacuo and in a vacuum followed by oxygen.

The redox properties of the iron in Fe-MCM-41 have been assessed by temperature-programmed reduction (TPR), and adsorption of NO has been studied by in situ infrared spectroscopy. Figure 2 shows TPR spectra of Fe-MCM-41 activated at 775 K either in nitrogen or in air. The main feature after pretreatment in air is a broad hydrogen consumption peak centered at 639 K. The area under the peak represents 0.8 hydrogen atoms per iron atom, as indicated in Table 1. The sample pretreated in nitrogen showed a peak in a similar position, with a hydrogen consumption of ca. 0.5 H/Fe. In addition to this peak, a hydrogen evolution feature was observed at 995 K, with an area equivalent to 1 H/Fe. The evolution peak most likely results from methoxy species, which will be discussed in a subsequent communication.[29]

Nitric oxide adsorption is an informative method of studying the redox behavior of these materials, as NO interacts strongly with Fe(II) species, but only weakly with Fe(III).[30] All infrared bands due to NO result from interaction with iron, since no NO stretching vibration bands were observed when an MCM-41 sample pretreated in vacuo, but containing no iron, was exposed to 10 mbar NO at 305 K. Figure 3 compares spectra for NO adsorption on Fe-MCM-41 following pretreatment in

TABLE 2: EXAFS Data of Samples Pretreated in Different Atmospheres[a]

	r(Fe−O)	N(Fe−O) (σ^2)	r(Fe−Fe)	N(Fe−Fe) (σ^2)	r(Fe−Si)	N(Fe−Si) (σ^2)
Fe-MCM-41 as prep.	1.96	4.4 (0.019)	2.61	0.5 (0.013)	3.27	3.6 (0.025)
Fe-MCM-41(N_2)	1.94	3.9 (0.031)	2.56	0.2 (0.0001)	3.26	1.7 (0.014)
Fe-MCM-41 synthesis (N_2)	1.92	4.0 (0.028)	−	−	3.26	2.0 (0.022)
Fe-MCM-41 (N_2, H_2)	1.97	3.4 (0.031)	2.63	0.2 (0.0001)	3.25	2.0 (0.037)

[a] See text for conditions. Distances (r) given in Å, Debye−Waller factors (σ^2) in Å^2.

vacuo at 775 K, or in vacuo and after exposure to oxygen. Much more NO is adsorbed on the vacuum treated material, indicating the presence of significant quantities of Fe(II). After oxidation as described above, followed by reduction at 675 K in hydrogen, similar concentrations of NO could be adsorbed as on a sample pretreated in a vacuum. Both the TPR results and these changes in NO adsorption capacity, dependent on whether the pretreatment atmosphere is oxidizing or reducing, show clearly that the oxidation state of the iron is easily varied between Fe(II) and Fe(III). This is analogous to the behavior observed for iron[8] and copper[10] *exchanged* into the zeolite ZSM-5.

The nature and structure of the iron species present has been probed by X-ray absorption spectroscopy. Figure 4 shows real space and reciprocal space iron K-edge EXAFS spectra of Fe-MCM-41 materials, with parameters for the best fit between experimental and calculated reciprocal space spectra given in Table 2. The figure also includes, for comparison, spectra of hematite (Fe_2O_3). The MCM-41 spectra, irrespective of pretreatment conditions, are dominated by an iron−oxygen distance of 1.95 ± 0.02 Å, with a coordination number of ca. 4. This distance is similar to the average of those observed when iron is exchanged into H-ZSM-5, but significantly longer than the Fe−O distance of 1.86 Å reported for iron within a silicalite framework[31] and somewhat longer than the average value of 1.92 Å that we have found for iron introduced into the MCM-41 framework during synthesis (Table 2).[32]

Table 2 indicates the presence of an Fe−Fe interatomic distance of ca. 2.6 Å, similar to the very short distance that we have noted for iron−oxo *nanoclusters* in Fe-ZSM-5. Statistical testing[33] shows that this feature is significant, even though the coordination numbers are very low, typically 0.2 in the activated samples.

The only other feature of significance in the Fourier transform EXAFS spectra occurs at an interatomic distance of just above 3 Å, and the best fit to the experimental data (reciprocal space spectrum) is achieved by introducing a silicon neighbor at 3.26 ± 0.01 Å. The identification of only oxygen and silicon as neighbors of the iron species strongly suggests that the transition metal cations are isolated from each other. To probe the extent to which this material may contain iron−oxo clusters, it is important to examine whether there could also be a contribution to this peak in the Fourier transform from iron−iron interatomic distances. When an iron shell is introduced instead of an Fe−Si distance, the best fit is achieved with a coordination number of 1.7 and an interatomic distance of 3.05 Å. However, the fitting index[33] is significantly worse than is observed for the Fe−Si interatomic distance. When the optimization program is invited to fit both Fe−Si and Fe−Fe interatomic distances at the same time, it shows a marked preference for the Fe−Si distance. We thus believe that the main neighbors for iron atoms in MCM-41 are oxygen and silicon, indicating that the iron species are present in the form of isolated atoms.

If this shell of neighbors does include some iron as well as silicon, any iron−oxo clusters present must be very small. Bulk iron oxides are relatively dense, and the next nearest neighbor, Fe−Fe peak in the Fourier transform EXAFS spectrum of hematite shown in Figure 4 contains contributions from a total of 9 atoms. The low coordination number observed for Fe-MCM-41 indicates that the average size of any iron-containing clusters present in these materials is no more than thus 5 Å in diameter. It should also be noted that these iron−oxo nanoclusters would have a structure quite different from those with the very short iron−iron interatomic distance of ca. 2.5−2.6 Å.[8]

The adsorption of nitric oxide on Fe-MCM-41 is also expected to provide evidence on the nature of the iron species present, particularly by comparison with NO/Fe-ZSM-5 interactions we have described in detail in ref 8, where the assignment of bands is also discussed. Figure 5 shows infrared spectra for adsorption on a vacuum-activated sample. At low pressures, the dominant absorption peak is at 1823 cm^{-1}, and we believe that this corresponds to the band at 1841 cm^{-1}, which we have reported for Fe-ZSM-5 and attributed to isolated iron ions. The band due to adsorption of NO on iron−oxo nanoclusters in Fe-ZSM-5 occurs at a much higher frequency of 1880 cm^{-1}.[8]

The shift of 18 cm^{-1} compared to the band due to adsorption on isolated species in Fe-ZSM-5 is due to the higher acidity of Fe-ZSM-5, due to the presence of aluminum sites. The tetrahedral aluminum near to the transition metal ion, compared to the silicon present in MCM-41, results in a higher positive effective charge on the iron. When NO binds to the iron site, this higher charge leads to a greater degree of interaction of the lone antibonding electron in the HOMO of NO with the iron ion, which in turn results in a higher frequency for the NO stretch.[34] At higher pressures of NO, bands are found at 1608 and 1590 cm^{-1}, which are attributed to the presence of NO_2 and nitrate species formed by NO disproportionation.

We now consider how the iron cations bind to the internal surface of the mesoporous MCM-41. The strong interaction of the MCM-41 with methanol is also interesting, but will be discussed elsewhere.[29] Purely siliceous MCM-41, despite having no charge balancing species of the sort found in crystalline aluminosilicates, appears to have a high uptake capacity for iron. EXAFS indicates that the iron cations are multiply coordinated to oxygen, with silicon as the predominant next nearest neighbors, suggesting that iron cations are held at silanol nests at the MCM-41 internal walls. Infrared spectroscopy suggests that the density of these nests is high in MCM-41 (Figure 1), certainly much higher than is found in well-crystallized zeolites, and this is of course in character with the less ordered and less stable nature of the MCM-41 materials. The infrared spectra shown in Figure 1 indicate that introduction of iron causes a significant reduction in the intensity of the silanol nest −OH feature, which is consistent with our proposal. The XANES spectra provide little information on the environment of the iron cations. There is a weak, pre-edge feature at 7104.3 eV, similar to that seen in Fe-ZSM-5, but none of the samples studied show the strong XANES pre-edge peak at 7104.0 eV, which is indicative of a tetrahedral iron and which is seen in compounds such as iron(III) phosphate and iron in the MCM-41 and silicalite framework.[35] Even though the EXAFS results suggest that the predominant iron environment is four-coordinate, this is not surprising, since even slight deviations from tetrahedral symmetry result in a strong reduction in the intensity of this pre-

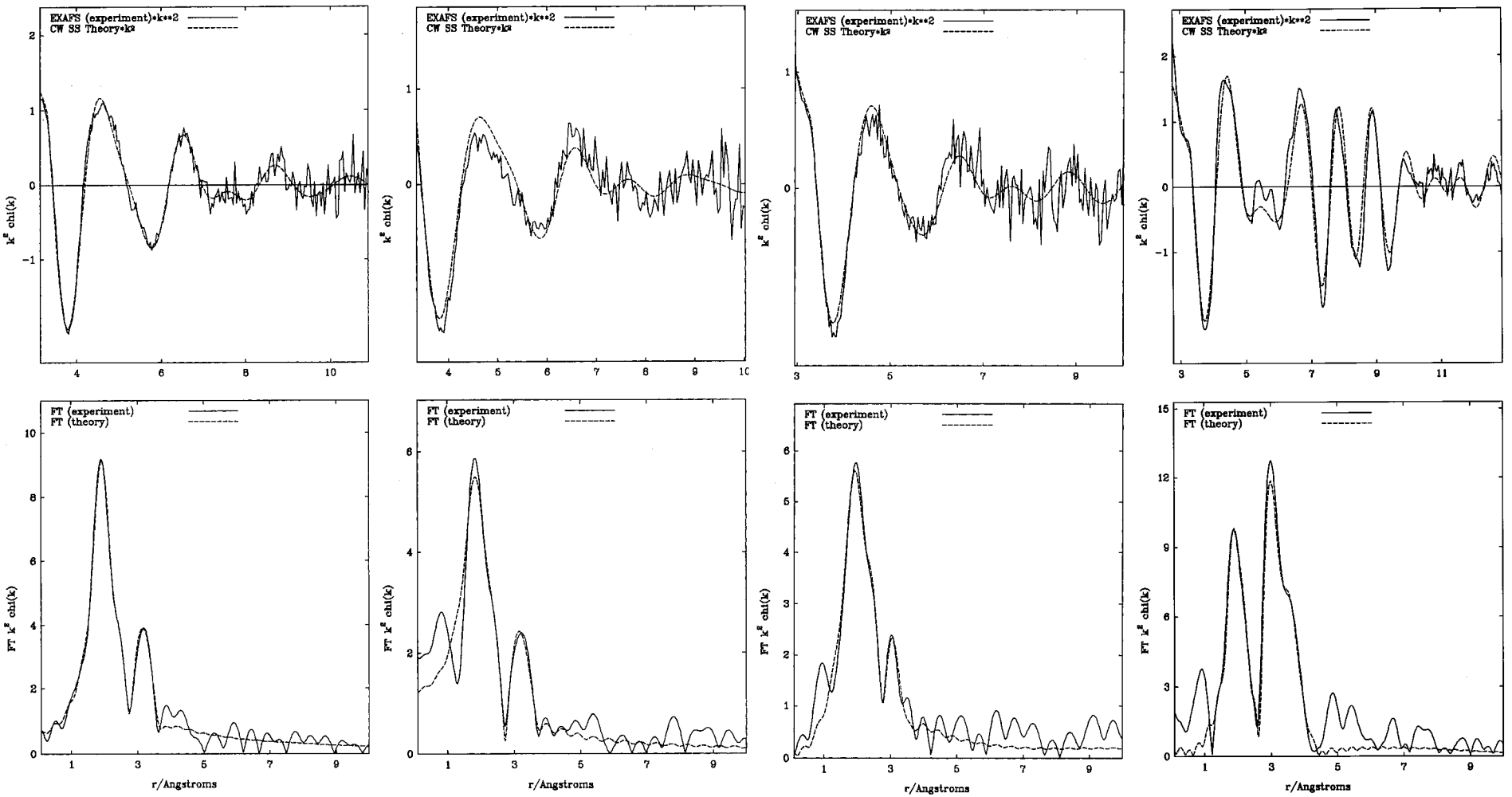

Figure 4. Experimental (solid line) and calculated (dashed line) reciprocal space and real space (Fourier transform) EXAFS spectra (left to right): (a) prepared Fe-MCM-41; (b) as before but after in situ heating in nitrogen at 655 K; (c) as in (b) but after subsequent heating in hydrogen at 655 K; (d) Fe_2O_3. The parameters used in the calculations are listed in Table 2.

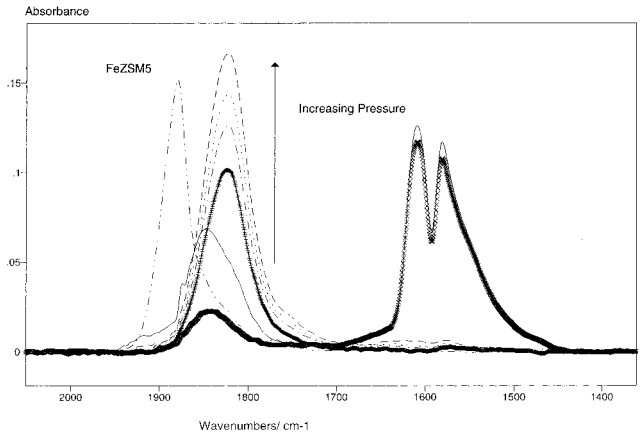

Figure 5. Infrared spectra as a function of pressure for the adsorption of nitric oxide on Fe-MCM-41, pretreated in vacuo at 775 K: (vertical crosses) 10^{-3} mbar; (dashed/dotted line) 10^{-2} mbar; (dotted line) 10^{-1} mbar; (dashed line) 1 mbar NO; (solid line) 10 mbar; (diagonal crosses) the irreversibly bound NO remaining after pumping at 305 K for 150 min. For comparison, a labeled spectrum obtained at 10^{-2} mbar for NO adsorbed on Fe-ZSM-5 at is also shown (from ref 8).

edge peak[36] and the MCM-41 environment is expected to be rather disordered, particularly where there are silanol nests.

The combination of the oxygen nearest neighbors and the absence of exchangeable cations shows that iron introduction into MCM-41 probably involves bonding with a covalent component, rather than the largely electrostatic interaction that characterizes ion exchange. As a result, there are both similarities and differences between the behavior of iron in ZSM-5[8] and in MCM-41. In both cases there is facile interchange between Fe(II) and Fe(III) but high stability against reduction to the metallic state. In ZSM-5, iron exists both as isolated cations and in the form of nanoclusters with the typical composition Fe_4O_4 and very short iron−iron interatomic distances, while predominantly isolated ions occur in MCM-41. Although the uptake capacity for iron is significantly greater in MCM-41, catalytic performance is inferior to that of Fe-ZSM-5, when the latter is correctly activated. Detailed catalytic studies will be presented elsewhere, but the activity of Fe-MCM-41 in the selective catalytic reduction of NO_x by propene in the presence of oxygen is about one-quarter that of the best Fe-ZSM-5 materials. Using hydrogen as reductant, however, at 575 K, 6% NO conversion was observed, which is significantly better than that with most Fe-ZSM-5 materials. Oxidation of cyclododecane with N_2O over Fe-MCM-41 resulted in dehydrogenation to cyclododecene. Cyclohexane oxidation over Fe-ZSM5 on the other hand, leads mainly to formation of oxygenated products, like alcohols and epoxides. Details of the catalytic data will be given elsewhere.[32]

4. Conclusions

Exposure to a methanolic solution of iron(III) nitrate followed by high-temperature activation leads to the introduction of substantial quantities of iron into a purely siliceous MCM-41. The methanol solvent also interacts with the mesoporous solid, forming highly stable methoxy species. Iron is introduced in the form of isolated species, which exhibit facile interchange of Fe(II)/Fe(III), similar to Fe-ZSM-5. The most significant difference between Fe-MCM-41 and Fe-ZSM-5 materials is the type of iron species formed. Fe-ZSM-5 contains, depending on the preparation procedure, large proportions of Fe_4O_4 *nanoclusters*, whereas in Fe-MCM-41 the predominant species are isolated cations. Over these different species, quite different catalysis was observed in a number of test reactions.

NO is strongly adsorbed at the iron cations, resulting in a broad infrared band at 1823 cm^{-1}. At NO pressures greater than 1 mbar the adsorbed species disproportionate, forming inter alia surface nitrate species.

Acknowledgment. We wish to thank Dr. J. Hargreaves and Dr. A. Dent for their help with EXAFS measurements and Dr. O. Tkachenko for her help with EXAFS and TPR measurements. We also wish to thank Dr. P. Trens for the synthesis of the original MCM41 material. The Chemical Database Service at Daresbury Laboratories is gratefully acknowledged as well as the EPSRC for funding.

References and Notes

(1) See e.g.: Panov, G. I.; Sobolev, V. I.; Dubkov, K. A.; Kharitonov, A. S. *Stud. Surf. Sci. Catal.* **1996**, *101*, 493.
(2) Anderson, J. R.; Tsai, P. *J. Chem. Soc., Chem. Commun*. **1987**, 1435.
(3) Feng, X.; Hall, W. K. *Catal. Lett.* **1996**, *41*, 45.
(4) Chen, H. Y.; Sachtler, W. M. H. *Catal. Today* **1998**, *42*, 73.
(5) Feng, X. B.; Hall, W. K. *Catal. Lett.* **1996**, *41*, 45.
(6) Chen, H. Y.; Voskoboinikov, T.; Sachtler, W. M. H. *J. Catal.* **1998**, *180*, 171.
(7) Joyner, R. W.; Stockenhuber, M. *Catal. Lett.* **1997**, *45*, 15.
(8) Joyner, R. W.; Stockenhuber, M. *J. Phys. Chem. B* **1999**, *103*, 5963.
(9) Panov, G. *Appl. Catal. A−General* **1995**, *123*, N14.
(10) Grunert, W.; Hayes, N. W.; Joyner, R. W.; Shpiro, E. S.; Siddiqui, M. R. H.; Baeva, G. N. *J. Phys. Chem.* **1994**, *98*, 10832.
(11) Bordiga, S.; Buzzoni, F.; Geobaldo, F.; Lamberti, C.; Giamello, E.; Zecchina, A, Leofanti, G.; Petrini, G.; Tozzola, G.; Vlaic, G. *J. Catal.* **1996**, *158*, 486.
(12) Morice, J. A.; Rees, L. V. A. *Trans. Faraday Soc*. **1968**, *64*, 1388.
(13) Lazar, K.; Palborbely, G.; Beyer, H. K.; Karge, H. G. *J. Chem. Soc., Faraday Trans.* **1994**, *90*, 1329.
(14) Karge, H. G.; Zhang, Y.; Beyer, H. K. *Catal. Lett.* **1992**, *12*, 147.
(15) Sachtler, W. M. H. *Catal. Today* **1992**, *15*, 419.
(16) Lersch, P.; Bandermann, F. *Appl. Catal.* **1991**, *75*, 133.
(17) Jentys, A.; Pham, N. H.; Vinek, H.; Englisch, M.; Lercher; J. A. *Catal. Today* **1998**, *39*, 311.
(18) Djajanti, S. D.; Howe, R. F. *Stud. Surf. Science Catal.* **1997**, *105*, 2067.
(19) He, N.; Bao, B.; Xu, Q. *Stud. Surf. Sci. Catal.* **1997,** *105***,** 85.
(20) Schiesser, W.; Vinek, H.; Jentys, A. *Catal. Lett.* **1998**, *56*, 189.
(21) Verhoef, M. J.; Kooyman, P. J.; Peters, J. A.; vanBekkum, H. *Micropor. Mesopor. Mater*. **1999**, *27*, 365.
(22) Vercruysse, K. A.; Klingeleers, D. M.; Colling, T.; Jacobs, P. A. *Stud. Surf. Sci. Catal*. **1998**, *117*, 469.
(23) Zhao, X. S.; Audsley, F.; Lu, G. Q. *J. Phys Chem. B* **1998**, *102*, 4143.
(24) Grün, M.; Unger, K. K.; Matsumoto, A.; Tsutsumi, K. In *Characterisation of Porous Solids IV*; McEnanney, B., Mays, T. J., Rouqueroul, R., Sing, K. S. W., Unger, K. K., Eds.; Royal Society of Chemistry: London, 1997.
(25) Hudson, M. J.; Trens, P.; Denoyel, J. *J. Mater. Chem.* **1998**, *8*, 2147.
(26) Jentys, A.; Pham, N. H.; Vinek, H. *J. Chem. Soc., Faraday Trans.* **1996**, *92*, 3287.
(27) Mirth, G.; Lercher, J. A.; Anderson, M. W.; Klinowski, J. *J. Chem. Soc., Faraday Trans.* **1990**, *86*, 3039.
(28) Nakamoto, K. *Infrared and Raman Spectra of Inorganic and Coordination Compounds*, 4th ed.; John Wiley and Sons: New York, 1986.
(29) Joyner, R. W.; Stockenhuber, M. Manuscript in preparation.
(30) Davydoff, A. A. *Infrared Spectroscopy of Adsorbed Species on the Surface of Transition Metal Oxides*; John Wiley and Sons: New York, 1990.
(31) Axon, S. A.; Fox, K. K.; Carr, S. W.; Klinowski, J. *Chem. Phys. Lett.* **1992**, *189*, 1.
(32) Grubert, G.; Joyner, R. W.; Stockenhuber, M. Manuscript in preparation.
(33) Joyner, RW.; Martin, K. J.; Meehan, P. *J. Phys. C.* **1987**, *20*, 4005.
(34) Hadjiivanov, K; Saussey, J.; Freysz, J. L.; Lavalley, J. C. *Catal. Lett.* **1998**, *52*, 103.
(35) Rey, F.; Sankar, G. T. Maschmeyer, T.; Thomas, J. M.; Bell, R. G.; Greaves, G. N. *Topics in Catalysis* **1996**, 3, 121.
(36) Bordiga, S.; Geobaldo, F.; Lamberti, C.; Zecchina, A.; Boscherini, F.; Genoni, F.; Leofanti, G.; Petrini, G.; Padovan, M.; Gerremia, S.; Vlaic, G. *Nucl. Instrum. Methods Phys. Res. B* **1995**, *97*, 23.